Theoretical and computational study of internal motions in some small molecules

Vesa Hänninen
University of Helsinki
Department of Chemistry
Laboratory of Physical Chemistry
P.O. BOX 55 (A.I. Virtasen aukio 1)
FIN-00014 University of Helsinki, Finland

Academic dissertation

To be presented, with the permission of the Faculty of Science of the University of Helsinki for public criticism in the Main lecture hall A110 of the Department of Chemistry (A.I. Virtasen aukio 1, Helsinki) May 25th, 2004, at 12 o'clock.

Helsinki 2004

Supervised by:
Professor Lauri Halonen
Department of Chemistry
University of Helsinki

Reviewed by:
Professor Kari Laasonen
Department of Physical Chemistry
University of Oulu
and
Professor Matti Hotokka
Department of Physical Chemistry
Åbo Akademi

Discussed with:
Professor Luciano Fusina
Dipartimento di Chimica Fisica e Inorganica
University of Bologna
Italy

ISBN 952-91-7242-7 (nid.)
ISBN 952-10-1864-X (PDF)
http://ethesis.helsinki.fi
Helsinki 2004
Yliopistopaino

Abstract

This work contains studies in theoretical and computational spectroscopy of methanol, partially deuterated silane, and bismutine. Vibrational spectra of methanol have been simulated in the fundamental, first C-H stretching overtone, and O-H stretching overtone regions using both normal and local mode models. A vibration-torsion local mode model based on curvilinear internal coordinates has been employed to find a physical interpretation for torsionally splitted vibrational energy levels of methanol. A high-level *ab initio* quartic anharmonic force field for methanol has been computed and used in the calculation of normal mode spectroscopic parameters with perturbation theory. Ro-vibrational spectroscopic parameters for the near local mode stretching states of H_3SiD have been calculated from an *ab initio* force field and applied to the analysis of high-resolution Fourier transform infrared and laser-photoacoustic spectra. Corrections to the bond stretching kinetic energy coefficients have been calculated due to the presence of rigid constraints in the bending degrees of freedom for C_{3v} pyramidal molecules stibine, ammonia, bismutine, and arsine. Stretching vibrational overtone spectra of bismutine have been analyzed with a simple stretching vibrational local mode model.

Contents

List of publications

1. V. Hänninen, M. Horn, and L. Halonen, Torsional motion and vibrational spectroscopy of methanol. J. Chem. Phys. **111**, 3018 (1999).

2. A. Miani, V. Hänninen, M. Horn, and L. Halonen, Anharmonic force field of methanol. Mol. Phys. **98**, 1737 (2000).

3. H. Bürger, M. Lecoutre, T. R. Huet, J. Breidung, W. Thiel, V. Hänninen, and L. Halonen, The (n,0,0), n = 3, 4, and 6, local mode states of H_3SiD: Fourier transform infrared and laser-photoacustic spectra and *ab initio* calculations of specroscopic parameters. J. Chem. Phys. **114,** 8844 (2001).

4. V. Hänninen, and L. Halonen, Calculation of spectroscopic parameters and vibrational overtones of methanol. Mol. Phys. **101**, 2907 (2003).

5. W. Jerzembeck, H. Bürger, V. Hänninen, and L. Halonen, First stretching overtone of BiH_3: An extreme local-mode case for XH_3-type molecule? J. Chem. Phys. **120**, 5650 (2004).

1 Introduction

There has been rapid development in the methods of molecular spectroscopy in recent years. Fast computers are available for theoretical calculations, and new lasers and sensitive detection techniques have been introduced for experiments. It has become possible to obtain more and more accurate information about molecules and molecular processes at microscopic scale. Internal molecular motions can be studied experimentally with optical spectroscopy, because electromagnetic radiation can be used to excite and access appropriate quantum states. Theoretical advances in this context are mainly consentrated on the development of methods of electronic structure calculations and on methods to treat nuclear motion.

Internal molecular motions of nuclei can be characterized as rotations, vibrations, and large amplitude motions. Molecular vibration occurs when the motions of nuclei are localized around the potential energy minimum. Most familiar vibrations are bond stretchings and bond angle bendings, which give rise to common examples of so-called zeroth order vibrational states. In the case of large amplitude motion, such as torsion, inversion, etc., where the motion extends over more than one potential energy minimum, a simple zeroth order picture is not valid. However, in reality, the states usually contain character of different motions due to kinetic and potential energy couplings. In spite of this, it is useful to label the vibrational states as stretching and bending vibrations, for example, as these often describe well the physical nature of the true states.

Molecular potential energy surfaces, obtained as solutions of electronic Schrödinger equations, play a key role in molecular physics. For example, chemical reactions, molecular shapes, vibration-rotation spectra, and intramolecular energy flow are dependent on the molecular force field. Potential energy surfaces can be obtained by using empirical and theoretical, so called *ab initio* methods. Empirical force fields are typically expressed as analytic functions, such as Taylor or Fourier series expansions, where coefficients are determined using experimentally observed ro-vibrational spectra as data. Theoretical potential energy surfaces can be computed accurately with *ab initio* electronic structure calculations.

Møller-Plesset second-order (MP2) and fourth-order (without triple corrections to energy: MP4(SDQ)) [1]) perturbation theory and coupled-cluster (CCSD (T) [2]) *ab initio* electronic structure calculation methods are commonly used in quantum chemistry. In the perturbation theory method, solution to the electronic

Schrödinger equation is approached in a systematic fashion by an order-by-order expansion of the wave function and energy. Perturbation theory provides accurate and profitable (in the sense of time consumption) approach in practical calculations. However, in many cases, even higher precision is required. The coupled-cluster approach is capable of providing highly accurate solutions to the electronic correlation problem. The drawback is the high computational cost of coupled-cluster wave functions. In the CCSD method, the electron single and douple excitations are treated by coupled cluster theory. In the CCSD(T) method, the CCSD calculation is improved by adding most important triple corrections in a perturbative fashion.

Internal vibrational energy redistribution (IVR) [3] is an example of an interesting phenomenom that is linked to potential energy surfaces obtained with the above-mentioned theoretical quantum chemistry methods. The dynamical flow of vibrational energy after a light pulse exitation or molecular collisions can lead to interesting consequences. It has been speculated that some unimolecular reactions are dependent on vibrational dynamics and thus could be controlled by laser excitations. For example, interesting results have been achieved in terminal acetylenes [4], where the calculations predict extended lifetimes of non-stationary C-H stretching states. However, it seems that the timescale of IVR in most systems is several orders faster than the timescale of chemical reactions. This hinders the hope of laser controlled chemistry in a large scale.

Despite the rapid development of theoretical methods in molecular science, majority of data comes from experiments. Theoretical results are often tested by comparison to experimental data. In optical spectroscopy, the ro-vibrational state of a molecule changes either by absorbing or emitting light, or by collisions. The energies of the transitions are measured with sophisticated spectroscopic techniques, which, for example, include the use of laser and Fourier transform infrared spectroscopy. The experimentally observed spectra provide molecular data such as vibrational energies, transition moments, and spectroscopic parameters. Time dependent methods are used to probe dynamical molecular processes, such as chemical reactions.

Vibrational problems of polyatomic molecules are not usually solvable excactly. In practice this means that approximations are employed. Pertubation theory and variational methods are two of the most common methods used in quantum chemistry. For example, perturbation theory can provide vibrational model parameters from an *ab initio* force field. Variational methods can be

employed to find solutions to vibrational problems by optimizing variational coefficients.

The choice of vibrational coordinates is usually problem dependent. The standard normal mode approach [5] is often a practical way to calculate vibrational fundamental energies of stretchings and bendings. The methods based on curvilinear bond stretch- bond angle bend internal coordinates, used, for example, in local mode models [6, 7, 8], have been applied successfully to calculate overtone spectra of small hydrides. The internal coordinate approach seems to be a good way to model interactions between high-frequency vibrations and large amplitude motions [9].

This work includes a series of studies that apply the standard normal mode and the local mode theories to model and calculate vibrational spectra and spectroscopic parameters for methanol, partially deuterated silane, and bismutine. The main emphasis of this thesis is on theoretical spectroscopic studies of the methanol molecule. It is an interesting species being the smallest molecule with an internal methyl rotor and thus it provides a model system to study interactions between high-frequency vibrations and the large amplitude internal rotation. It is a sufficiently small system for accurate *ab initio* force field calculations. Moreover, rich experimental vibrational overtone spectra have been recorded for methanol [11, 12, 13, 14]. This makes it feasible to test theoretical approaches.

In Paper 1, a vibration-torsion model was employed to calculate and interpretate torsionally splitted O-H stretching overtone spectra of methanol. The non-linear least squares method was used to obtain model parameters using experimentally observed vibrational term values as data. Some of the model parameters were estimated using a torsionally dependent harmonic force field calculated by *ab initio* methods. The model was successfully used to interpretate spectral features such as decreasing torsional splittings in high overtones. The standard deviation of the fit between calculated and observed vibrational term values was 2.9 cm^{-1}, which is a good result taking into account the experimental uncertainties.

In Paper 2, an *ab initio* quartic anharmonic force field for methanol was calculated in the bond stretch- bond angle bend internal coordinate representation at the equilibrium position. Several *ab initio* methods were tested in order to simulate experimental vibrational spectra of methanol isotopomers CH_3OH, CH_3OD, CD_3OH, and CD_3OD in the fundamental region. The best agreement with observed fundamental term values was found using the coupled-cluster

CCSD(T)/VTZ [15, 16] method for the structure and harmonic potential energy surface and the Møller-Plesset fourth order perturbation theory MP4(SDQ)/AVTZ [15, 16] method for the anharmonic part of the surface. The standard cc-pVTZ (noted as VTZ above) basis and a modified aug-cc-pVTZ (noted as AVTZ above) basis were employed in all computations. Vibrational calculations were carried out using standard normal mode theory devoting special care to the inclusion of cubic anharmonic Fermi resonance interactions between different vibrational states. In the calculation of fundamentals for all isotopomers, the mean absolute error of 5.8 cm^{-1} was achieved, which is good, considering that the large amplitude torsional mode was included in the calculation just as a small amplitude degree of freedom.

In Paper 3, the experimental rovibrational spectrum of H_3SiD in the first, second, and fourth stretching overtone states was studied with the normal mode and local mode models. Arithmetic normal-local mode parameter relations were used in assigning the spectroscopic transitions. Hamiltonian coefficients were calculated from the experimental spectra and compared to values obtained from an *ab initio* force field. It was necessary to use *ab initio* data in determining some of the model parameters.

In Paper 4, the vibrational spectra of methanol were simulated with a normal mode model, where the torsion is excluded. The model was employed to calculate spectra at O-H stretching overtone regions up to the sixth overtone and at the first C-H stretching overtone region. The force field computed in Paper 2 was extensively used in these calculations. Most of the model parameters were fixed to the *ab initio* values. The non-linear least squares method was adopted to optimize some of the parameters in order to achieve a satisfactory fit between the calculated and observed vibrational term values. New assignments for the observed vibrational bands at the first C-H stretching overtone region were proposed.

In Paper 5, stretching vibrational energies were calculated for BiH_3 assuming that the bond angle bending displacement coordinates were constrained to the equilibrium values. The method for modifying vibrational kinetic energy coefficients in the presence of rigid constraints was adopted in the calculation of model parameters. The effect of setting rigid constraints to bending motion, was found to be neglible in the case of stretching vibrational energies.

2 Force field calculations of methanol

Accurate potential energy surfaces are vital in modelling molecular vibrational motion. Two different approaches can be adopted in obtaining force fields. First, experimental data are used to determine empirical force fields, which are expressed in terms of empirical model parameters. This method is sensitive to the quality and amount of experimental data. It is obvious that the number of independent potential energy parameters cannot exceed the number of experimentally observed transitions. This sets restrictions to the model. It can be difficult even to determine the force field ambiguously. This can lead to situations, where the physical interpretation of the model parameters is uncertain. Second, *ab initio* methods can be employed to obtain theoretical force fields. The coefficients of analytic potential energy surface can be computed from a numerical potential energy grid where the energies have been calculated at the grid points by *ab initio* methods. Despite the power of modern computers, high-level *ab initio* computations can be time consuming even for small molecules. Thus, data obtained from electronic structure calculations are often not enough to produce accurate vibrational or rovibrational energy levels when compared with experimental spectra. It can still be necessary to employ empirical methods in vibrational problems. The results in Papers 1 and 4 show that for a challenging molecule like methanol, the best surfaces are obtained by combining experiment and theory.

The equilibrium and saddle point geometries and the force field of methanol have been calculated with various methods including Møller-Plesset perturbation theory MP2, MP4(SDQ)/AVTZ and coupled cluster CCSD(T)/VTZ *ab initio* methods. The torsional motion is treated as a small amplitude vibration around the potential energy minimum. Thus, the amount of computations is sufficiently small to employ expensive, time consuming methods. Considering, that the energies of torsional splittings associated with the vibrational transitions are small, the force field is valid for the high-frequency vibrational motions. Methanol possesses C_s point group symmetry in the equilibrium configuration. The potential energy surface has been expressed as a function of symmetrized stretching and bond angle displacement internal coordinates. A set of these coordinates is defined as follows,

$$S_1 = \Delta r_{CO} \tag{1}$$

$$S_2 = \Delta r_{OH} \tag{2}$$

$$S_3 = \frac{1}{\sqrt{3}} (\Delta r_1 + \Delta r_2 + \Delta r_3) \tag{3}$$

$$S_4 = \frac{1}{\sqrt{6}} (2\Delta r_1 - \Delta r_2 - \Delta r_3) \tag{4}$$

$$S_5 = \Delta\varphi \tag{5}$$

$$S_6 = \frac{1}{\sqrt{6}} (\Delta\beta_1 + \Delta\beta_2 + \Delta\beta_3 - \Delta\alpha_1 - \Delta\alpha_2 - \Delta\alpha_3) \tag{6}$$

$$S_7 = \frac{1}{\sqrt{6}} (2\Delta\alpha_1 - \Delta\alpha_2 - \Delta\alpha_3) \tag{7}$$

$$S_8 = \frac{1}{\sqrt{6}} (2\Delta\beta_1 - \Delta\beta_2 - \Delta\beta_3) \tag{8}$$

$$S_9 = \frac{1}{\sqrt{2}} (\Delta r_2 - \Delta r_3) \tag{9}$$

$$S_{10} = \frac{1}{\sqrt{2}} (\Delta\alpha_2 - \Delta\alpha_3) \tag{10}$$

$$S_{11} = \frac{1}{\sqrt{2}} (\Delta\beta_2 - \Delta\beta_3) \tag{11}$$

$$S_{12} = \Delta\tau, \tag{12}$$

where r_{CO} is C-O bond stretching, r_{OH} is O-H bond stretching, r_1, r_2, and r_3 are C-H bond stretchings, φ is C-O-H bond angle bending, α and β variables are H-C-H and H-C-O bond angle bendings, respectively, τ is a torsional coordinate, which is defined as a dihedral angle between r_{OH} and r_1, and the symbol Δ denotes a displacement from an appropriate equilibrium value.

Force fields have been obtained by displacing the appropriate atoms along the symmetry coordinates and fitting the total calculated energies with quadratic polynomials by the linear least-squares method. The anharmonic force fields have been expressed in series expansions around equilibrium configurations with force constants F as coeffients, i.e.

$$V(S_1, S_2, ..., S_{12}) = \sum_{ij} F_{ij} S_i S_j + \sum_{ijk} F_{ijk} S_i S_j S_k + \sum_{ijkl} F_{ijkl} S_i S_j S_k S_l + ..., \tag{13}$$

where unrestricted summations are over all twelve vibrational degrees of freedom.

3 Vibrational models

The vibrational models used in this work are based on conventional normal coordinates and on curvilinear internal coordinates. In literature, these methods are usually referred as normal mode [5] and local mode models [7, 17, 18], respectively. Both approaches possess theoretical and/or practical benefits, depending on the molecular system. It would be advantageous if the model coordinates reflected the physical nature of the oscillators. For example, the local mode description of the X-H bond stretching overtone levels provides a simpler and physically better approach than the normal mode picture does. It seems that curvilinear internal coordinates give a better basis for the treatment of large amplitude motions. In methanol, local mode models have been successfully applied to simulate the vibration-torsion spectra for C-H stretching states [9]. On the other hand, for some molecules, the spectrum is characteristically normal. In SO_2, for example, the origin of the strong interbond coupling arises from kinetic energy and leads to a spectrum which shows normal mode behavior. However, there are drawbacks in the conventional method. By definition, the normal coordinates are rectilinear [10], which is not accurate especially in the description of large amplitude motions. Additionally, normal coordinates are nuclear mass dependent, causing potential energy surfaces expressed in terms of these coordinates to be isotope non-invariant.

The number of the vibrational states may become large in vibrational overtone calculations of polyatomic molecules. Therefore, it is not always possible to employ full variational calculations. The size of the Hamiltonian matrix can be reduced by employing the method of block diagonal Hamiltonians. In this approach, a good quantum number, which is a linear combination of the quantum numbers of the zeroth order states, is defined. Only the states that possess the same good quantum number are coupled.

3.1 Normal mode model

Standard normal mode theory is based on the concept of rectilinear normal coordinates, which are obtained from internal coordinates by finding a transformation which removes the harmonic cross terms both in the force field and kinetic energy. Hamiltonian coefficients, spectroscopic parameters such as harmonic wave numbers, anharmonicity constants, and resonance coefficients, can be calculated

from the force field using perturbation theory.

The standard equation for the diagonal elements in the vibrational Hamiltonian matrix of an asymmetric rotor is [5]

$$\langle \upsilon_r \left| H/hc \right| \upsilon_r \rangle = \sum_r \omega_r \left(\upsilon_r + \frac{1}{2} \right) + \sum_{r \leq s} x_{rs} \left(\upsilon_r + \frac{1}{2} \right) \left(\upsilon_s + \frac{1}{2} \right). \qquad (14)$$

The summation indices in Eq. (14) are over all normal modes, υ_r is the vibrational quantum number of the rth mode, ω_r parameters are the harmonic normal mode wave numbers, and the anharmonicity parameters x_{rs} are known algebraic functions of the structure, harmonic wave numbers, Coriolis coupling coefficients, and cubic and semi-diagonal quartic force constants. As usual, h is Planck's constant and c is the velocity of light.

In practice, Eq. (14) is inadequate in calculating vibrational term values accurately in molecules where anharmonic resonances, such as Fermi and Darling-Dennison interactions, are present. Fermi resonance occurs, for example, when a state including one quantum of high-frequency vibrational mode ν_r is close in energy with an overtone state $2\nu_s$ or a combination state $\nu_s + \nu_t$ which contain two quanta of lower frequency vibrational mode/modes. Fermi resonance matrix elements [19] for an asymmetric rotor are

$$\begin{aligned} & \langle \upsilon_r, \upsilon_s, \upsilon_t \left| H_{Fermi}/hc \right| \upsilon_r - 1, \upsilon_s + 1, \upsilon_t + 1 \rangle \\ = \; & \langle \upsilon_r, \upsilon_s, \upsilon_t \left| \phi_{rst} q_r q_s q_t \right| \upsilon_r - 1, \upsilon_s + 1, \upsilon_t + 1 \rangle \\ = \; & \phi_{rst} [\upsilon_r (\upsilon_s + 1)(\upsilon_t + 1)/8]^{1/2} \end{aligned} \qquad (15)$$

$$\begin{aligned} & \langle \upsilon_r, \upsilon_u \left| H_{Fermi}/hc \right| \upsilon_r - 1, \upsilon_u + 2 \rangle \\ = \; & \left\langle \upsilon_r, \upsilon_u \left| \frac{1}{2} \phi_{ruu} q_r q_u^2 \right| \upsilon_r - 1, \upsilon_u + 2 \right\rangle \\ = \; & \frac{1}{2} \phi_{ruu} [\upsilon_r (\upsilon_u + 1)(\upsilon_u + 2)/8]^{1/2}. \end{aligned} \qquad (16)$$

The anharmonicity parameters x in equation (14) are replaced by modified constants x^*, which exclude those second order perturbation theory contributions that are included explicitly in the Fermi resonance model. Thus, in the case of

resonances given in Eqs. (15) and (16), the required relationships are [20, 21]

$$\begin{aligned} x_{rs} &= x^*_{rs} + \phi^2_{rst}/[8(\omega_r - \omega_s - \omega_t)] \\ x_{rt} &= x^*_{rt} + \phi^2_{rst}/[8(\omega_r - \omega_s - \omega_t)] \\ x_{st} &= x^*_{st} - \phi^2_{rst}/[8(\omega_r - \omega_s - \omega_t)] \\ x_{ru} &= x^*_{ru} + \phi^2_{ruu}/[8(\omega_r - 2\omega_u)] \\ x_{uu} &= x^*_{uu} - \phi^2_{ruu}/[32(\omega_r - 2\omega_u)]. \end{aligned} \tag{17}$$

Darling–Dennison resonance terms [22, 23] stem from quartic anharmonicities in the force field. As an example, in water, these resonances arise between pairs of states such as $2\nu_1$ and $2\nu_3$ where ν_1 and ν_3 are the symmetric and antisymmetric stretching fundamentals, respectively. In the case of an asymmetric rotor, Darling–Dennison resonance matrix elements are defined as [24, 25, 26]

$$\langle \upsilon_r, \upsilon_s \,|H_{D-D}/hc|\, \upsilon_r - 2, \upsilon_s + 2\rangle = \frac{1}{4} K_{rrss}[\upsilon_r(\upsilon_r - 1)(\upsilon_s + 1)(\upsilon_s + 2)]^{1/2} \tag{18}$$

$$\begin{aligned} \langle \upsilon_r, \upsilon_s \,|H_{D-D}/hc|\, \upsilon_r - 1, \upsilon_s + 1\rangle &= \frac{1}{4}[3K_{rrrs}\upsilon_r + 3K_{rsss}(\upsilon_s + 1) \\ &\quad + \sum_{t \neq r,s} 2K_{rtst}(\upsilon_t + \frac{1}{2})][\upsilon_r(\upsilon_s + 1)]^{1/2} \end{aligned} \tag{19}$$

$$\langle \upsilon_r, \upsilon_s, \upsilon_t \,|H_{D-D}/hc|\, \upsilon_r - 2, \upsilon_s + 1, \upsilon_t + 1\rangle = \frac{1}{4} K_{rrst}[\upsilon_r(\upsilon_r - 1)(\upsilon_s + 1)(\upsilon_t + 1)]^{1/2}, \tag{20}$$

where K_{rrss}, K_{rrrs}, K_{rsss}, K_{rtst}, and K_{rrst} are the resonance coefficients.

3.2 Local mode model

In the local mode models, [6, 7, 8] the vibrational Hamiltonian is expressed in terms of curvilinear bond stretch/bond angle internal displacement coordinates. Coupled Morse oscillator Hamiltonians [27] are employed to describe the stretching vibrations. This approach is similar in spirit to normal mode models although details and physical interpretation of the Hamiltonian coefficients differ. There are some advantages using the curvilinear internal coordinate approach. For example, the physical picture of the model is clear and intuitive, and the potential energy surfaces are isotope invariant. Moreover, curvilinear internal coordinates provide a more accurate representation of potental energy functions than rectilinear coordinates [28].

The diagonal elements of the stretching vibrational Hamiltonian can be calculated using the equation

$$\langle \upsilon_r \left| H/hc \right| \upsilon_r \rangle = \sum_r \left[\omega_r' \left(\upsilon_r + \frac{1}{2} \right) + x_{rr} \left(\upsilon_r + \frac{1}{2} \right)^2 \right], \tag{21}$$

where the summation index r is over the stretching vibrational modes, υ_r is the vibrational quantum number of the rth stretching mode, ω_r' includes the harmonic wave number $\omega_r = \hbar \left(2a_r^2 D_e g^{(rr)} \right)^{1/2} / (hc) = \hbar \left(f_{rr} g^{(rr)} \right)^{1/2} / (hc)$ and small perturbation corrections that arise from $\Delta\upsilon = \pm 2$ couplings [8], and $x_{rr} = -a_r^2 \hbar^2 g^{(rr)} / (2hc)$ is the bond anharmonicity parameter. The Morse dissociation energy D_e, the Morse steepnes parameter a_r, and the harmonic constant $f_{rr} = \left(\frac{\partial^2 V}{\partial q_r^2} \right)_e$ are potential energy parameters. The quantity $g^{(rr)} = \frac{1}{m_X} + \frac{1}{m_Y}$ is a kinetic energy coefficient, where m_X and m_Y are the masses of nuclei X and Y. Formally, Hamiltonians similar to Eq. (21) can also be used for bond angle bending oscillators.

The stretching oscillators are coupled to each other by bilinear kinetic and potential energy terms. The off-diagonal matrix element that couple the states are

$$\langle \upsilon_r, \upsilon_{r'} \left| H/hc \right| \upsilon_r + 1, \upsilon_{r'} - 1 \rangle = \lambda \left[\left(\upsilon_r + 1 \right) \upsilon_{r'} \right]^{1/2}, \tag{22}$$

where

$$\lambda = \frac{1}{2} \omega_r \left(\frac{g_e^{(rr')}}{g^{(rr')}} + \frac{f_{rr'}}{f_{rr}} \right), \tag{23}$$

where the coefficients are defined as $f_{rr'} = \left(\frac{\partial^2 V}{\partial q_r \partial q_{r'}} \right)_e$ and $g_e^{(rr')} = \frac{\cos\theta_e}{m_X}$. If the bending degrees of freedom are included in the model, theoretical interpretations of the parameters in Eqs. (21) - (23) slightly change as there are more perturbative corrections [8].

In the internal coordinate formulation, Fermi resonance matrix elements are defined as

$$\langle \upsilon_r, \upsilon_\theta, \upsilon_{\theta'} \left| H_{Fermi}/hc \right| \upsilon_r - 1, \upsilon_\theta + 1, \upsilon_{\theta'} + 1 \rangle = \frac{1}{2} \phi_{r\theta\theta'} [\upsilon_r (\upsilon_\theta + 1)(\upsilon_{\theta'} + 1)/8]^{1/2} \tag{24}$$

$$\langle \upsilon_r, \upsilon_\theta \left| H_{Fermi}/hc \right| \upsilon_r - 1, \upsilon_\theta + 2 \rangle = \frac{1}{2} \phi_{r\theta\theta} [\upsilon_r (\upsilon_\theta + 1)(\upsilon_\theta + 2)/8]^{1/2}, \tag{25}$$

where the physical interpretation of the resonance coefficients $\phi_{r\theta\theta'}$ and $\phi_{r\theta\theta}$ differ from the conventional normal mode model force constants [8].

3.3 Local modes and vibration-torsion interaction in methanol

In methanol, the fundamental transition energies of bond stretchings, bond angle bendings, and rockings occur in a higher energy region than the lowest transition energies of the large amplitude torsional mode. Thus, high-energy modes can be assumed to be adiabatically separable from the torsional degree of freedom. Within the adiabatic approximation, kinetic and potential energy terms of high-energy modes are defined at a given torsional angle. Thus,

$$H = \sum_{i}^{n} H(p_i, q_i, \tau) + H_{tor}, \tag{26}$$

where the index i is over all n vibrational degrees of freedom other than the torsion, q_i is the displacement coordinate of the ith vibrational mode and p_i is its conjugate momentum, τ is the torsional coordinate, and the torsional Hamiltonian is

$$H_{tor}/hc = \frac{F}{\hbar^2} j^2 + \frac{1}{2} V_3 (1 - \cos 3\tau) + \frac{1}{2} V_6 (1 - \cos 6\tau). \tag{27}$$

The coefficient F is the ground state inertial constant of the torsional motion, j is the torsional angular momentum operator, and V_3 and V_6 are Fourier coefficients of the torsional potential. The torsional potential in methanol possesses three equivalent minima as the molecule contains three equilibrium configurations along the torsional coordinate. Thus, the torsional coordinate must meet the requirement that the potential reaches the minimum when the torsional coordinate possess the values $\tau = \frac{2\pi k}{3} + C$, where $k = 0, 1, 2, ...$ and C is an arbitrary constant. None of the dihedral angles of methanol (see Figure 1) fullfill this requirement because the H-C-H bond angles do not remain unchanged during the torsional motion. In my work, the torsional angle is defined as

$$\tau = \frac{1}{3} \left(3\pi - \alpha - \beta - \gamma\right), \tag{28}$$

where α, β, and γ are dihedral angles (see Figure 1).

In my vibration-torsion model, spectroscopic parameters, which are functions of kinetic and potential energy coefficients, are expanded as Fourier series using the torsional angle as an expansion coordinate [9]. Thus,

$$g = g_0 + g_l \cos l(\tau + \phi) + ... \tag{29}$$

$$f = f_0 + f_l \cos l(\tau + \phi) + ... \ . \tag{30}$$

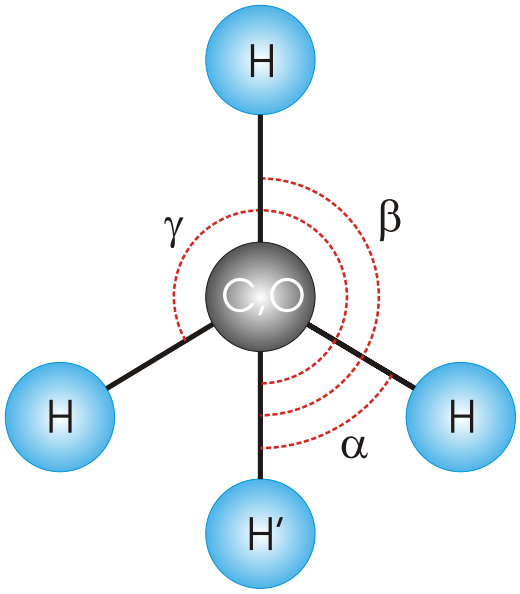

Figure 1: Dihedral angles of methanol

The Hamiltonian is periodic with respect to the torsional angle $2\pi/l$. The quantity ϕ is a phase angle. When higher order terms in the expansions are omitted, the vibration-torsion interaction Hamiltonian can be arranged in torsionally independent and dependent parts, i.e.,

$$H^{(0)} = \frac{1}{2}(g_0 p^2 + f_0 q^2) \tag{31}$$

$$H^{(l)} = \frac{1}{2}\left[g_l \cos l(\tau+\phi)p^2 + f_l \cos l(\tau+\phi)q^2\right]. \tag{32}$$

The Hamiltonians given are expressed conviniently using shift operators which are defined as

$$a^+ = \frac{1}{\sqrt{2}}\left(\alpha^{1/2}q - i\alpha^{-1/2}\hbar^{-1}p\right) \tag{33}$$

$$a = \frac{1}{\sqrt{2}}\left(\alpha^{1/2}q + i\alpha^{-1/2}\hbar^{-1}p\right), \tag{34}$$

where

$$\alpha = \frac{1}{\hbar}\sqrt{\frac{f_0}{g_0}} = \frac{2\pi c\omega}{\hbar g_0} \tag{35}$$

and ω is the harmonic wave number. The shift operators operate on the harmonic oscillator eigenfunctions as

$$a^+ |\upsilon\rangle = \sqrt{\upsilon+1}\,|\upsilon+1\rangle \tag{36}$$

$$a\,|\upsilon\rangle = \sqrt{\upsilon}\,|\upsilon - 1\rangle\,, \tag{37}$$

where υ is the vibrational quantum number. The torsionally dependent Hamiltonian operator of Eq. (32) can be written as

$$H^{(l)}/hc = \frac{\omega}{4}\left(\frac{g_l}{g_0} + \frac{f_l}{f_0}\right)\cos l(\tau+\phi)\left(aa^+ + a^+a\right) = \mu_l \cos l(\tau+\phi)\left(aa^+ + a^+a\right). \tag{38}$$

4 Calculation of vibrational term values of methanol

Methanol is an ideal model system to study vibration-torsion interactions. The large amplitude torsional motion causes splittings in the spectrum. Some approximations are needed in order to analyze the experimentally observed rich band structure. The O-H and C-H stretching vibrations can be separately accessed by vibrational overtone excitations. Thus, the vibrational spectrum of methanol can be qualitatively described in terms of motion in two different groups. This is useful in model calculations. First, the O-H stretching states, which are observed as strong peaks up to the sixth overtone, are mostly not mixed with other states. The origin of the generally weak interactions comes from a relatively large energy separation of the O-H stretching states from the states of the other modes. However, there are some interesting exceptions that are discussed later. Second, the methyl group including the three C-H bond stretching, three H-C-H bending, and two H-C-O rocking modes forms a set of strongly coupled oscillators that show complicated band systems in the spectrum.

This work contains a detailed analysis of most of the experimentally assigned vibrational term values of methanol. New assignments for the bands occurring in the first C-H stretching overtone region are proposed for the first time. However, some observed bands in the higher C-H stretching overtones are difficult to assign due to the high density of states. No effort has been made to analyse these spectral regions. Normal and local mode models have been used to study interesting structures shown in the experimental spectra in order to obtain information about associated vibrational dynamics between the interacting states.

The conventional normal mode model has been used to calculate methanol spectra at the fundamental, C-H first overtone, and O-H overtone regions. Torsion has been treated as a small amplitude motion and thus the model adopted does not produce torsional splittings associated with the vibrational transitions.

All model parameters have been calculated initially from the force field (Paper 2). Allthought the *ab initio* force field produces the spectra accurately at the fundamental region, the non-linear least squares optimization method was needed in the simulation of overtone spectra.

A local mode model was adopted in the calculation of the vibration-torsion spectra of methanol. The least squares optimization method was employed to determine the majority of the parameters. The torsional dependancy of some of the model parameters was calculated by *ab initio* methods.

4.1 Fundamental region

Vibrational spectra of methanol were calculated for various isotopic species of methanol in the fundamental region. All modes including the low energy torsional mode were included in calculations. However, all vibrations were treated as small amplitude motions around the equilibrium position.

As a first step, the program Spectro [29] was employed to calculate normal mode harmonic wave numbers and anharmonicity parameters from the quartic anharmonic force field. In the second step, vibrational term values were calculated employing a program written by Andrea Miani. This modifies the values of anharmonicity parameters obtained in the first step by taking into account Fermi resonances. All Fermi resonance interactions within a specified energy separation ϵ between levels were included in the calculation. The CCSD(T)/VTZ harmonic wave numbers were used to estimate whether the possible interacting states are within the gap ϵ. Different sets of anharmonicity parameters and associated vibrational energies were produced by varying ϵ systematically from 0 up to 1000 cm^{-1}. As expected, the vibrational energies converged for large values of ϵ, although anharmonicity parameters still change.

4.1.1 Fundamentals of CH_3OH

Fundamentals of CH_3OH were calculated using the MP2/VTZ, MP4(SDQ)/AVTZ, CCSD(T)/VTZ, and CCSD(T)/AVTZ sets of harmonic wave numbers, and the MP4(SDQ)/AVTZ anharmonic parameters. The experimental values are shown in Table 1 together with respective C_s point group symmetries and descriptions. Comparison between the experimental and calculated fundamental term values are shown in Table 7 of paper 2. The best set of calculated fundamentals is

obtained using the harmonic wave numbers of the CCSD(T) method with the VTZ basis set. The mean absolute error between the experimental and the best calculated fundamentals is 5.0 cm^{-1}, when the torsion is included.

The fundamentals of the methyl group C-H stretching modes are strongly coupled with the exited states of low-energy modes via the Fermi resonance interaction. Calculations predict that the ν_3 vibrational mode is involved in the strongest Fermi interaction. The resonance occurs with the $2\nu_5$ state. When $\epsilon = 500$ cm^{-1}, the magnitude of the $2\nu_5$ wave function coefficient in the ν_3 vibrational state is 0.58 and the ν_3 contribution to the $2\nu_5$ overtone state is 0.38. Other significant contributions are given by $\nu_4+\nu_6$, $2\nu_{10}$, and $2\nu_4$. It is interesting to note that ν_3 is also mixed with states which are not interacting directly with it but which are involved in the Fermi interaction through other vibrations. The basis functions of these indirectly interacting coupled states possess coefficients in the ν_3 wavefunction. This indicates that it is also necessary to include indirectly interacting vibrational states to obtain accurate results. The ν_9 C-H stretching fundamental state is also significantly perturbed by the Fermi interaction. The largest contributions to the wave functions are already obtained considering states within 100 cm^{-1}. These turn out to be $\nu_4 + \nu_{10}$ and $\nu_5 + \nu_{10}$.

Table 1. Experimental fundamental term values of $^{12}CH_3OH$. All numbers are in cm^{-1}.

Mode	Sym.	Description	Wave number	Reference
ν_1	A′	O−H stretch	3693.9	[30]
ν_2	A′	C−H stretch	3007.0	[31]
ν_3	A′	C−H stretch	2844.7	[31]
ν_4	A′	H−C−H bend	1477.2	[32]
ν_5	A′	H−C−H bend	1454.5	[32]
ν_6	A′	C−O−H bend	1335.8	[32]
ν_7	A′	CH_3 rock	1074.5	[32]
ν_8	A′	C−O stretch	1033.8	[33]
ν_9	A″	C−H stretch	2966.7	[31]
ν_{10}	A″	H−C−H bend	1465.0	[32]
ν_{11}	A″	CH_3 rock	1145.0	[32]
ν_{12}	A″	torsion	271.5	[32]

4.1.2 Fundamentals of other isotopomers: CD_3OD, CD_3OH, and CH_3OD

The calculated fundamentals of CD_3OD, CD_3OH, and CH_3OD were obtained using the CCSD(T)/VTZ method for the structure and harmonic force field, and MP4(SDQ)/AVTZ for the anharmonic part of the potential energy surface. Experimental [32] and calculated fundamental term values are shown in Table 8 of paper 2. Fermi interactions up to the energy separation $\epsilon = 1000$ cm^{-1} were included in the calculations. The mean absolute errors between experimental and calculated fundamentals of CD_3OD, CD_3OH, and CH_3OD are 4.3 cm^{-1}, 6.0 cm^{-1}, and 7.9 cm^{-1}, respectively, when Fermi interactions were included in the model. The values for the experimental fundamentals are the average values of the torsionally splitted origins [32]. The only exception is the CD_3 rock ν_8 in CD_3OH, where the splitting is 15.7 cm^{-1}. This fundamental was not included in the calculation of the mean value. No experimental vibrational term value is available for the torsion of CH_3OD.

The most important Fermi interactions occurring in CD_3OD affect the C-D stretching fundamentals ν_2, ν_3, and ν_9. A similar observation has been made in the earlier section in the case of the C-H stretching fundamentals of CH_3OH. The main bending overtone and combination states involved in the interactions are $\nu_4+\nu_5$ and $\nu_4+\nu_6$ for ν_2, $\nu_5+\nu_7$, $2\nu_5$, $\nu_4+\nu_7$, and $2\nu_{10}$ for ν_3, and $\nu_5+\nu_{10}$, $\nu_4+\nu_{11}$, and $\nu_4+\nu_{10}$ for ν_9. The bending states listed for a particular stretching fundamental are given as decreasing importance as far as influencing the stretching state by resonance interactions are concerned.

The C-D stretching fundamentals ν_2 and ν_3, and the C-O-H bending fundamental ν_4 of CD_3OH are strongly affected by Fermi resonances, the most important interacting states being $\nu_5+\nu_6$ and $2\nu_5$ for ν_2, $2\nu_6$, $2\nu_{10}$, and $\nu_5+\nu_7$ for ν_3, and $\nu_{11}+\nu_{12}$ for ν_4.

The last isotopomer considered, CH_3OD, is the only one in which Fermi interactions affect ν_1, the O-D stretching fundamental. The main states giving rise to resonances are $2\nu_{10}$, $2\nu_5$, and $\nu_5+\nu_6$. The C-H stretching fundamental states ν_2 and ν_9 are affected by Fermi resonances to some extent as well. The most important states involved are $2\nu_5$ and $2\nu_4$ for ν_2, and $\nu_4+\nu_{10}$ and $\nu_5+\nu_{10}$ for ν_9.

4.2 C-H stretching first overtone region of CH_3OH

Vibrational spectra in the first C−H stretching vibrational overtone region of CH_3OH are complicated due to Fermi resonance interactions between the C−H stretching overtone/combination states and the low-frequency H−C−H and C−O−H bending, methyl rocking, and C−O stretching states. In the wave number range 5600–6000 cm^{-1}, experimental spectra (see Figure 2) show six bands [33] that are extensively broadened due to the high density of ro-vibrational states. The experimental spectra at higher overtone regions (C-H stretching quantum numbers greater than 2 in this work) show even broader band structures. I have not applied my models to these higher overtone regions.

The vibrational spectra of methanol have been calculated by employing a block diagonal normal mode model, which accounts for all Darling–Dennison resonances between the C−H stretching states and all Fermi resonances between the C−H stretching and low-frequency states. The appropriate spectroscopic parameters were taken from tables 2, 3, and 5 of Paper 4. The number of calculated vibrational states in the first C−H stretching overtone region is 300, which span the wave number region 4100–6000 cm^{-1}. The energies of the states that possess the highest percentage of the basis functions of the first C−H stretching overtones and combination states of $^{12}CH_3OH$ are included as a stick spectrum in Figure 2 . The energy values of these states are shown in table 7 of paper 4. The bands in experimental spectra (Figure 2 and Ref. [33]) are assigned as follows. The A band is $2\nu_3$, B consists of number of different bands including $\nu_3+\nu_9$, C is $\nu_2+\nu_3$ and $2\nu_9$, the weak band D is $\nu_2+2\nu_5$, E consists of $2\nu_2$ and $\nu_2+\nu_9$, and F is $\nu_2+\nu_4+\nu_5$. Intensity calculations are required to confirm this proposal but it seems that the relative intensities of the bands correlate to those observed in the fundamental region. For example, $2\nu_2$ might carry high intensity in the experimental spectra, because the fundamental ν_2 band is strong. Indeed, the band E is the strongest one in the experimental spectrum. Similarly, the ν_3 mode shows significantly smaller intensity than the other C-H stretching modes ν_2 and ν_9 [33]. This might indicate that $2\nu_3$ is a weak band as confirmed by the experimental spectrum. According to my calculations for the stretch-bend combination bands, $\nu_2+2\nu_5$ is mixed with $2\nu_2$ but to a lesser extent than $\nu_2+\nu_4+\nu_5$, pointing out that $\nu_2+2\nu_5$ might be weaker band than $\nu_2+\nu_4+\nu_5$. This again agrees with the experiment in the sense that F is stronger than D.

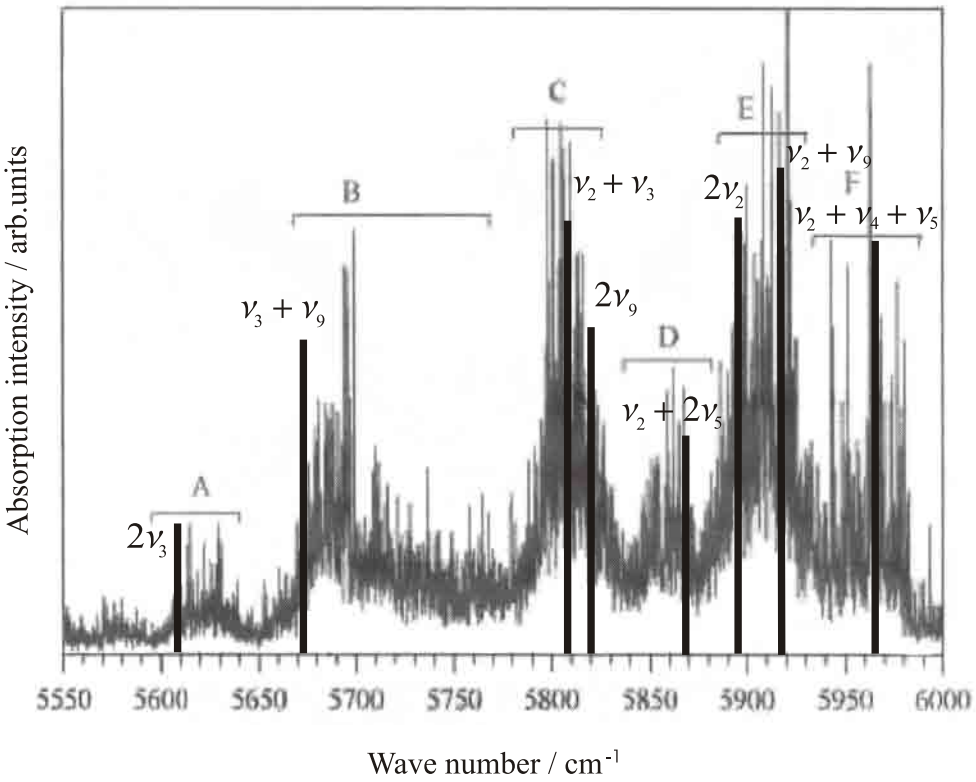

Figure 2: The methanol (CH_3OH) spectrum in the first C-H stretching overtone region. The calculated values are included as a stick spectrum. The intensities in the calculated stick spectrum are arbitrary (see discussion in the text).

4.3 O-H stretching overtone region of CH_3OH

Two different approaches were adopted in calculating methanol (CH_3OH) spectra in the O-H stretching vibrational overtone regions. In the model based on rectilinear normal coordinates (Paper 4), spectroscopic parameters were mainly obtained from the *ab initio* force field of Paper 2. Internal rotation of the O-H bond with respect to the methyl group was not allowed for in the normal mode model, and thus the torsion was treated as a small amplitude vibration. Independently, the local mode model based on curvilinear internal coordinates (Paper 1) was employed in order to study vibration-torsion interaction associated in the O-H stretching states. Internal rotation was allowed for in this approach. Both methods used experimental and *ab initio* data in the calculation of spectra. In the normal mode model, only 10 parameters from total of 173 needed to be optimized using observed vibrational term values as data. As far as the total number of parameters is concerned, the local mode approach is simpler: 19 of the total of 26 parameters were optimized.

Approximate block diagonal Hamiltonian methods have been employed both in the normal and local mode models. The models are further simplified by excluding weak couplings in the calculations. The coupling between various vibrational states in methanol is presented schematically in Figure 3.

In both approaches adopted in this work, the O-H stretching vibration is coupled to the C-H stretching vibration. The physical interpretation of the interaction differs. In the normal mode picture, the coupling is caused by Darling-Dennison resonance which contains quartic terms of the force field. In the local mode picture, the coupling is due to a harmonic potential energy cross-term.

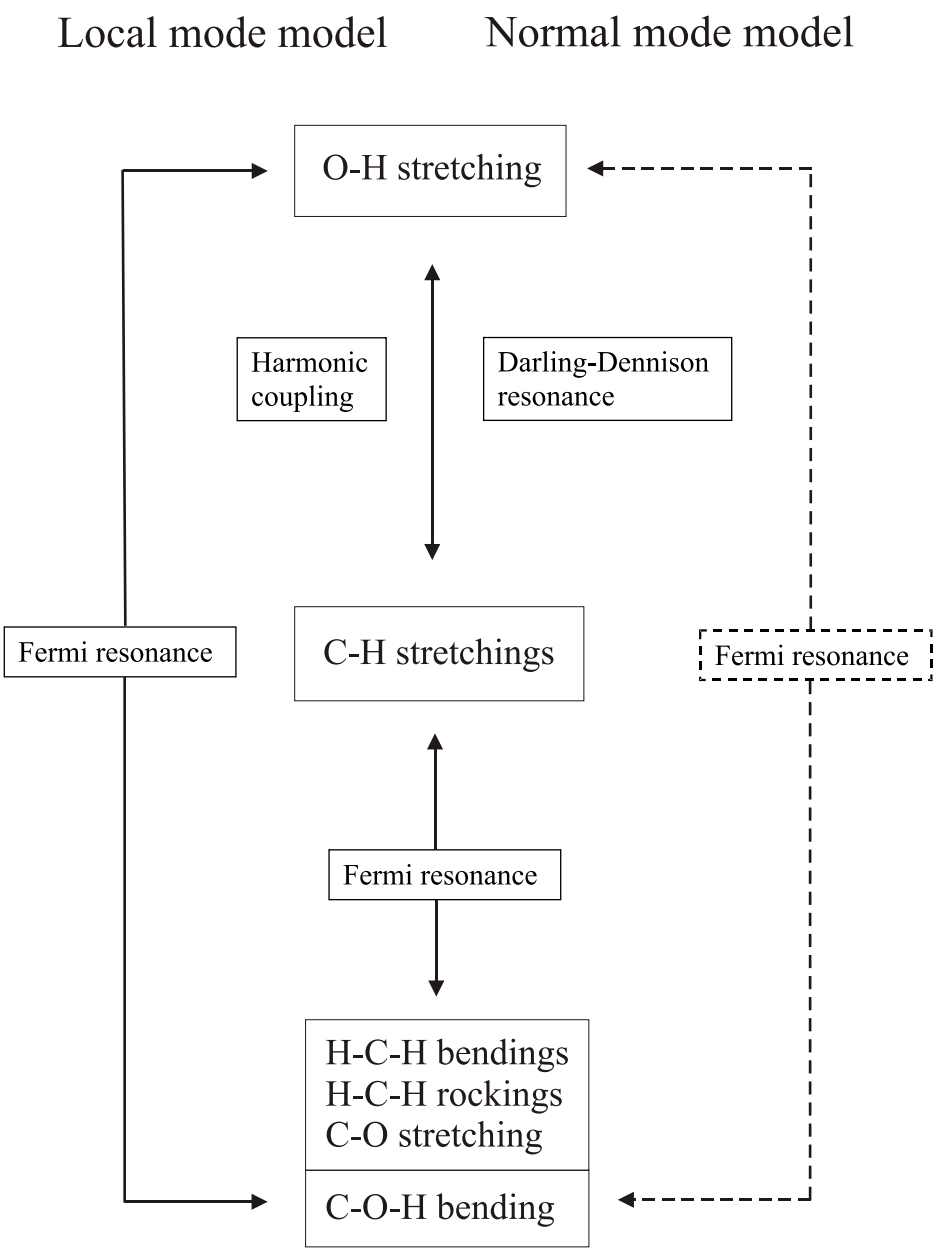

Figure 3: Coupling scheme for the O-H stretching mode of CH_3OH

4.3.1 Normal mode model calculations

The normal mode model of Eqs. (14) - (20) was employed in the calculation of the spectra of CH_3OH in the O-H stretching overtone regions. As a starting point, the spectroscopic parameters were calculated from the *ab initio* force field (Paper 2). However, it was found that this method did not produce vibrational spectra accurately at high overtones. Large deviations between experimental and calculated spectra arose at high energies ($\sim$ 100 cm^{-1} at 20 000 cm^{-1}) because errors in parameters ω_r and x_{rs} of Eq. (14) cumulated at high-energy quantum states. The calculation was improved by employing the non-linear least squares method to optimize a set of spectroscopic parameters. Because the number of observed states was limited, it was impossible to cover all different perturbations in the spectra by varying a larger set of parameters in order to obtain a better agreement with experiment. The set of parameters that were optimized contribute directly to many observed states and thus had a strong effect on calculated spectra. It was essential to vary harmonic wave numbers ω_1, ω_6, and ω_8 and anharmonicity parameters associated with the corresponding modes in order to achieve satisfactory results. It was, however, viable to use *ab initio* values for those parameters that possessed a secondary role in the spectral simulation. For example, the *ab initio* values of the H−C−H bending harmonic wave numbers could be used because these contribute only to a few observed low-lying states.

Calculated vibrational term values are shown in Table 4 of Paper 4 together with experimental gas phase values for $^{12}CH_3OH$ [33]. The mean absolute deviation between experimental and calculated values is 5.96 cm^{-1}, which is good considering that vibrational–torsional interaction causes dense structure which often cannot be rotationally resolved. Vibrational term values have been calculated using parameters shown in Table 5 and cubic anharmonic force constants shown in Table 2 in Paper 4. Most of the optimized parameters are close to the starting values obtained by *ab initio* calculations. This supports the conclusion that the quality of the potential energy surface used is good. A comparison between calculated and fitted parameters is shown in Table 6 of Paper 4.

Experimental spectra show some interesting features worth discussing. Interaction between the O−H and C−H stretching modes causes a striking 50 cm^{-1} splitting in the fourth O−H stretching overtone region and also appears as a larger splitting in the regions of the third and fifth O−H stretching overtones [11, 12, 13, 14]. The origin of the splittings was explained as a result of harmonic

coupling between the O−H stretching and unique C−H stretching oscillators in Ref. [34] and Paper 1 by models based on curvilinear internal coordinates. In this formulation, the coupling operator between the O−H and unique C−H bond oscillators includes only one spectral parameter. The physical picture is more complicated in models based on normal coordinates [35]. The coupling matrix element in Eq. (19), where $r = 1$ and $s = 2$, contains 12 parameters, $K_{1,1,1,2}$, $K_{1,1,1,3}$, and $K_{1,i,2,i}$, $i = 3, 4, ..., 12$, that contribute to the splitting. It is impossible to vary all these coefficients freely in the least squares optimization because the parameter set would become larger than the set of observed states. The parameter $K_{1,1,1,2}$ has the largest effect on the matrix element of Eq. (19) at high values of the O-H stretching quantum number υ_1. Therefore, it is reasonable to vary only one of the Darling–Dennison parameters which was chosen to be $K_{1,1,1,2}$. Its value changes from the *ab initio* value of 3.99 cm^{-1} to the fitted value of 4.05 cm^{-1}. This supports fully the approach adopted. The model reproduces spectra well in the third, fourth, and fifth O−H stretching overtone regions, where the mean absolute deviation between the experimental and calculated term values is close to 1.0 cm^{-1}.

The Fermi resonance interaction between the O–H stretching and C–O–H bending vibrations was not included in the model. This resonance can affect high O–H stetching overtone states. The calculated value of the $\phi_{1,6,6}$ Fermi resonance force constant, 433.70 cm^{-1} (see Paper 2), is large and cannot be used to reproduce the experimental spectrum at the sixth O–H stretching overtone region (see Table 4 of Paper 4 for the 100 cm^{-1}splitting between the $7\nu_1$ and $6\nu_1 + 2\nu_6$ states). Similar kind of difficulty in the internal coordinate representation was observed in Paper 1, where the corresponding Fermi resonance force constant determined from the experimental spectrum differed a lot from the *ab initio* value.

While the set of *ab initio* parameters produces good results for fundamental states, the least squares optimization method is required to obtain a satisfactory agreement with experimental spectra at high O−H stretching overtone regions. However, the model still relies heavily on *ab initio* results, as the number of freely optimized parameters is kept as small as possible. The values of spectroscopic parameters obtained are consistent with the results of previous works (Ref. [34] and Paper 1), which employed the least squares method with experimental vibrational term value data to determine internal coordinate model parameters.

4.3.2 Local mode model calculations

The O-H stretching overtone spectra of CH_3OH show interesting band structures. Particularly, the torsional tunneling splitting associated with O-H stretching vibrational states decreases as the overtone excitation increases. The effective torsional barrier depends on the O-H stretching vibrational quantum number in such a way that the barrier height increases at higher excitations. While models based on the standard normal mode theory are succesful in interpretating methanol spectra for small amplitude vibrations, it is not straightforward to extend these models to include the large amplitude torsional motion. Approaches based on curvilinear internal coordinates are suitable for this purpose [9]. The mathematical representation of vibration-torsion interaction is simple in the local mode picture. This approach has been succesfully applied to model vibration-torsion interactions at the C-H stretching fundamental region [9]. The same kind of approach is adopted for the O-H stretching region in my work.

Formally, the local mode model Hamiltonian is written as

$$\begin{aligned} H &= H_{CH} + H_{CH-CH} + H_{HCH} + H_{HCH-HCH} + H_{CH-HCH} + H_{OH} \\ &\quad + H_{OH-CH} + H_{COH} + H_{OH-COH} + H_{tor}, \end{aligned} \tag{39}$$

where, for example, H_{CH} represents the C-H stretching Hamiltonian and H_{CH-CH} contains harmonic interaction terms between the C-H stretching modes. The operator H_{tor} is the torsional Hamiltonian given in Eq. (27).

The eigenvalues of the Hamiltonian in Eq. (39) can be obtained variationally expressing the eigenfunctions as linear combinations of the product basis functions

$$|\upsilon_{r_1}\upsilon_{r_2}\upsilon_{r_3}, \upsilon_{\theta_1}\upsilon_{\theta_2}\upsilon_{\theta_3}, \upsilon_R, \upsilon_\varphi, m\rangle = |\upsilon_{r_1}\rangle\,|\upsilon_{r_2}\rangle\,|\upsilon_{r_3}\rangle\,|\upsilon_{\theta_1}\rangle\,|\upsilon_{\theta_2}\rangle\,|\upsilon_{\theta_3}\rangle\,|\upsilon_R\rangle\,|\upsilon_\varphi\rangle\,|m\rangle\,, \tag{40}$$

where the quantum labels $\upsilon_{r_i}, \upsilon_{\theta_i}, \upsilon_R$, and υ_φ refer to the ith C-H bond, ith H-C-H bond angle bending, O-H stretch, and C-O-H bending oscillators, respectively, and the quantum number m refers to free rotor states. In practice, full variational calculations would not produce converged eigenvalues for highly excited states, and it is necessary to adopt an approximate method, the block diagonal Hamiltonian model, where only states in strong resonance are coupled.

At high O-H stretching overtones, the vibrational dependancy of torsional inertia becomes signifigant. This has been taken into account in the model by

assuming that $F = F' - \upsilon_R F''$. The parameter F' is the vibrational ground state inertial constant for the torsional motion and the term $-\upsilon_R F''$ takes into account the experimentally observed O-H stretching vibrational excitation dependancy on the torsional inertial coefficient. The matrix elements of the torsional Hamiltonian are

$$\begin{aligned} & \langle \upsilon_R, m\acute{} | \, H_{tor}/hc \, | \upsilon_R, m \rangle \\ = & \left(Fm^2 + \frac{1}{2}V_3 + \frac{1}{2}V_6 \right) \delta_{m\acute{},m} - \frac{1}{4}V_3 \delta_{m\acute{}\pm 3,m} - \frac{1}{4}V_6 \delta_{m\acute{}\pm 6,m}. \end{aligned} \tag{41}$$

The O-H stretching vibrational Hamiltonian is

$$H_{OH} = \frac{1}{2}\left(g^{(RR)} p_r^2 + f_{RR} q_r^2 \right) + H_{anh}, \tag{42}$$

where on the right hand side the terms in brackets constitute the harmonic part and H_{anh} contains anharmonic potential energy terms. The coefficient $g^{(RR)} = g_e^{(RR)}$ is a constant but the harmonic force field parameter can be expressed as a Fourier series as

$$f_{RR} = f_{RR}^{(0)} + f_{RR}^{(3)} \cos 3\tau. \tag{43}$$

The anharmonic terms are assumed to be independent of the torsional angle. Thus, the torsionally dependent Hamiltonian (see Eq. (38)) takes the form

$$H_{OH}^{(3)}/hc = \mu_{RR} \cos 3\tau \left(aa^+ + a^+ a \right) \tag{44}$$

where

$$\mu_{RR} = \frac{\omega_R f_{RR}^{(3)}}{4 f_{RR}^{(0)}}.$$

The O-H stretching vibrational Hamiltonian gives rise to the following nonzero matrix elements

$$\begin{aligned} & \langle \upsilon_R, m\acute{} | \left(H_{OH}^{(0)} + H_{OH}^{(3)} \right) / hc \, | \upsilon_R, m \rangle \\ = & \left[\omega_R \upsilon_R + x_{RR} \upsilon_R \left(\upsilon_R + 1 \right) \right] \delta_{m\acute{},m} + \frac{2\upsilon_R + 1}{2} \mu_{RR} \delta_{m\acute{},m\pm 3}, \end{aligned} \tag{45}$$

where x_{RR} is the O-H stretching vibrational anharmonicity parameter.

In Paper 1, the model described was employed to simulate the experimental O-H stretching overtone spectra of methanol [11, 12, 13, 14]. The least squares method was used to optimize the model parameters to fit the experimental vibrational term values. Because of the limited amount of data available, it was

impossible to freely optimize all parameters and some of these were fixed to experimentally determined ground state values, like the torsional potential energy barrier coefficient V_3. *Ab initio* methods were also used to find good estimates for some of the parameter values, which were either fixed or used as a starting point for the predicate observations method [39]. The values of the model parameters are shown in Table 1 of Paper 1, and observed and calculated vibrational term values in Table 2 of Paper 1. The standard deviation of the fit obtained was 2.9 cm^{-1}.

The experimentally observed torsional splitting associated with the O-H stretching vibrational transitions shows decreasing tendency as the vibrational energy increases. This phenomenom can be explained in terms of my model in the following way. The torsional barrier height is mainly attributed to the coefficient V_3 in the ground vibrational state. In the model, in the O-H stretching Hamiltonian, the effective barrier height is attributed to the following coefficients in off-diagonal matrix elements:

$$\langle \upsilon_R, m \pm 3 | \left(H_{tor} + H_{OH}^{(3)} \right) / hc \, | \upsilon_R, m \rangle = -\frac{1}{4} V_3 + \frac{2\upsilon_R + 1}{2} \mu_{RR}. \qquad (46)$$

From Eq. (46), it is seen that the value of the matrix elements depends on the O-H stretching quantum number υ_R. Since the parameter μ_{RR} is negative, the effective torsional barrier increases in high O-H stretching overtone states. Part of the potential energy surface that describes the O-H stretching-torsion problem is

$$V(q_R, \tau)/hc = \frac{1}{2} f_{RR}^{(0)} q_R^2 / hc + f_{RR}^{(3)} q_R^2 \cos 3\tau / hc + \frac{1}{2} V_3 (1 - \cos 3\tau), \qquad (47)$$

where q_R is the O-H stretching displacement coordinate. The latter two terms in Eq. (47) contribute to the matrix element of Eq. (46). It can be seen in Figure 4, where the two-dimensional surface of Eq. (47) is plotted, how the effective torsional barrier increases by increasing q_R. At high stretching excitations, the wave function is spread out extending to higher q_R values than at low excitations. Thus, smaller splittings occur at high O-H stretching vibrational overtones.

The O-H stretching quantum number dependancy of the torsional inertia coefficient F also contributes to the decrease of the splittings. The term $-\upsilon_R F''$ decreases the value of the constant F and, thus, according to Eq. 41, decreases the energies of the vibration-torsion states by $-\upsilon_R F'' m^2$.

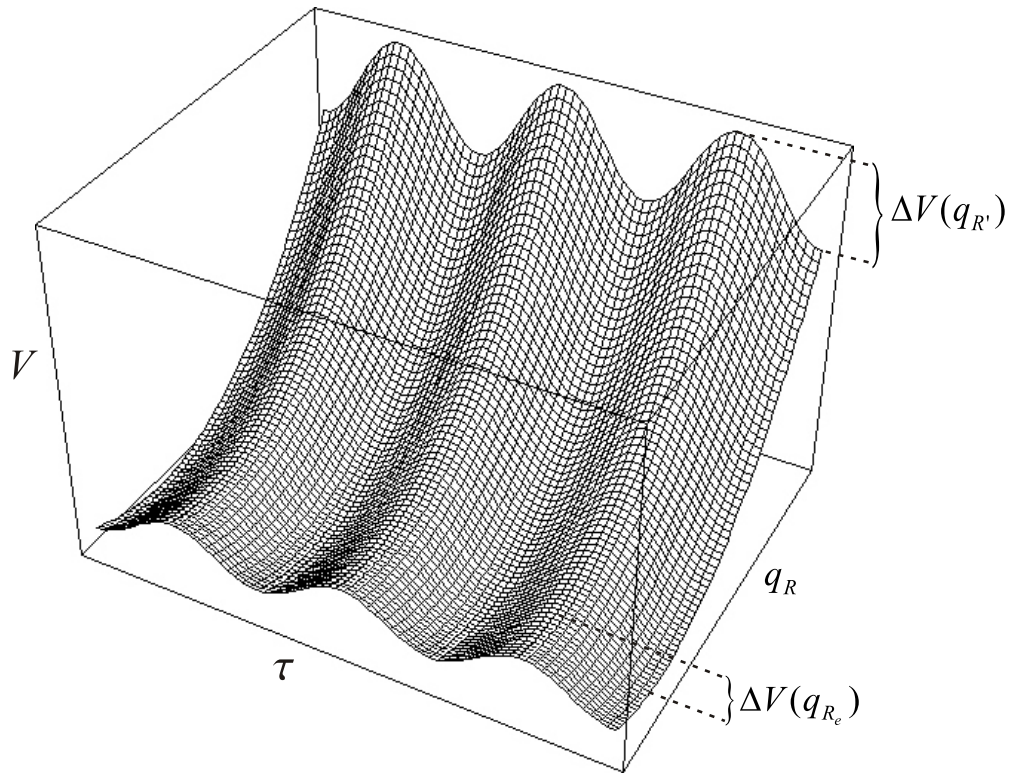

Figure 4: O-H stretching-torsion potential for CH_3OH. The quantity q_{R_e} is the equilibrium value of the O-H stretching coordinate and $q_{R'}$ is a specific point where the O-H stretching coordinate is extended from the equilibrium. The surface is presented schematically by exaggerating some of the model parameters (see Paper 1) and therefore the axes are given in arbitrary units.

5 Calculation of spectroscopic parameters of small C_{3v} symmetric top molecules

It is often beneficial to employ approximations in spectroscopic analyses. Sometimes there are not enough data (for example, experimental vibrational term values) to achieve good results. Approximations can reduce the work needed in the model calculations. The stretching vibrational states of some pyramidal hydrides show evidence of local mode behaviour. Therefore, the stretching states are effectively decoupled from each other and from bending states. The studies in Papers 3 and 5 include approximate models that employ the ideas of simple local mode models to the C_{3v} point group symmetric top molecules H_3SiD and BiH_3.

5.1 Calculations for H_3SiD

The experimental high-resolution spectrum of H_3SiD in the second (300)[1], third (400), and fifth (600) Si-H stretching overtone has been studied using the Fourier transform infrared technique for the two former bands and the laser-photoacoustic method for the latter. The recorded bands have been rotationally analyzed with a Hamiltonian model which uses simple arithmetic relations between some of the rovibrational parameters. The coefficients in the effective H_{22} Hamiltonian operator [36] have been calculated using an anharmonic *ab initio* force field and compared with experimental results. Moreover, these predictions have been used in cases where the spectroscopic data do not allow anambiguous determination of the parameters.

The model is based on the conventional vibration-rotation theory expressed in terms of normal coordinates. In this approach, there exist strong couplings between the rotational states belonging to A_1 and E vibrational states $(n00)$ which are almost degenerate. The Hamiltonian matrices are set up for each total angular quantum number J, and for the A_1, A_2, and E symmetry blocks using basis functions $|i, Jk\rangle = |i\rangle\,|Jk\rangle$. The quantum number k gives the angular momentum around the symmetry axis. The wave function $|i\rangle$ is a one-dimensional

[1]The states are given in the local mode notation [7] $(n00)$ which means that there are n quanta of stretching vibrational energy in one of the bond-oscillators and none in the other two bond-oscillators.

(A_1) or a two-dimensional (E) harmonic oscillator basis function expressed in terms of normal coordinates and $|Jk\rangle$ is a rigid rotor symmetric top eigenfunction. The diagonal matrix elements are
$[i = 000\ A_1\,(l=0)\,,\ n00\ A_1\,(l=0)\,,$ or $n00\ E\,(l=\pm 1)$ and $n \geq 1]$

$$\begin{aligned}\langle i, Jk\,|H/hc|\,i, Jk\rangle &= v_i + B_i J\,(J+1) + (A_i - B_i)\,k^2 - D_{Ji}J^2\,(J+1)^2 \\ &\quad -D_{JKi}J\,(J+1)\,k^2 - D_{Ki}k^4 + H_{Ji}J^3\,(J+1)^3 \\ &\quad -H_{JKi}J^2\,(J+1)^2\,k^2 + H_{KJi}J\,(J+1)\,k^4 \\ &\quad +H_{Ki}k^6 - A\zeta_i^{(z)}kl, \end{aligned} \tag{48}$$

where l is the vibrational angular momentum quantum number associated with the doubly degenerate vibration, A and B are rotational, and D and H are centrifugal distortion constants. The parameter $\zeta_i^{(z)}$ is the Coriolis coefficient for the doubly degenerate E state. The off-diagonal matrix elements consist α-resonance contributions,

$$\begin{aligned}&\langle n00\ E\,(l=+1)\,, Jk+1\,|H_{22}/hc|\,n00\ A_1, Jk\rangle \\ =\ &\langle n00\ A_1, Jk+1\,|H_{22}/hc|\,n00\ E\,(l=-1)\,, Jk\rangle \\ =\ &\frac{1}{2\sqrt{2}}\alpha_{eff}^{(AB)}\,(2k+1)\,F\,(J,k)\end{aligned} \tag{49}$$

and

$$\begin{aligned}&\langle n00\ E\,(l=-1)\,, Jk+2\,|H_{22}/hc|\,n00\ A_1, Jk\rangle \\ =\ &\langle n00\ A_1, Jk+2\,|H_{22}/hc|\,n00\ E\,(l=+1)\,, Jk\rangle \\ =\ &\frac{1}{2\sqrt{2}}\alpha_{eff}^{(BB)}F\,(J,k)\,F\,(J,k+1)\,,\end{aligned} \tag{50}$$

l-resonance contribution,

$$\begin{aligned}&\langle n00\ E\,(l=+1)\,, Jk+2\,|H_{22}/hc|\,n00\ E\,(l=-1)\,, Jk\rangle \\ =\ &-\frac{1}{2}q_{eff}F\,(J,k)\,F\,(J,k+1)\,,\end{aligned} \tag{51}$$

and r-resonance contribution,

$$\begin{aligned}&\langle n00\ E\,(l=-1)\,, Jk+1\,|H_{22}/hc|\,n00\ E\,(l=+1)\,, Jk\rangle \\ =\ &2r_{eff}\,(2k+1)\,F\,(J,k)\,,\end{aligned} \tag{52}$$

with

$$F\,(J,k) = [J\,(J+1) - k\,(k+1)]^{1/2}\,. \tag{53}$$

The coefficients $\alpha_{eff}^{(AB)}$, $\alpha_{eff}^{(BB)}$, q_{eff}, and r_{eff} describe the strength of the appropriate interactions. The interpretation of the effective molecular parameters given can be obtained with the standard normal mode model based on the inclusion of quartic anharmonic Darling-Dennison resonance between stretching states [37, 38].

The band systems (300), (400), and (600) were rotationally analyzed with the model given above. For some cases, for example in the band system (300), the parameters $\alpha_{eff}^{(AB)}$ and r_{eff} were poorly determined, if spectroscopic parameters were optimized freely using experimental vibration-rotation spectra as data. Therefore, these coefficients were constrained to values obtained from *ab initio* predictions. The same procedure was also followed in the band systems (400) and (600).

At high stretching exitations, silane is close to the rovibrational local mode limit as the bond oscillators become effectively vibrationally and rotationally decoupled. In this circumstance, there exist simple arithmetic relations between the effective spectroscopic parameters [40]. If these are combined with the results in Refs. [41] and [42], the following relations are obtained:

$$A_0 - A_{n00} = \frac{n}{3}\left(\alpha_1^{(A)} + 2\alpha_4^{(A)}\right) \tag{54}$$

$$B_0 - B_{n00} = \frac{n}{3}\left(\alpha_1^{(B)} + 2\alpha_4^{(B)}\right) \tag{55}$$

$$q_{eff} = -\frac{1}{\sqrt{2}}\alpha_{eff}^{(BB)} = \frac{n}{3}\left(\overline{q}_4 - \sqrt{2}\alpha_{14}^{(BB)}\right) \tag{56}$$

$$r_{eff} = \frac{1}{4\sqrt{2}}\alpha_{eff}^{(AB)} = \frac{n}{6}\left(2r_4 - \frac{1}{\sqrt{2}}\alpha_{14}^{(AB)}\right). \tag{57}$$

The parameters A_0 and B_0 are the ground state rotational constants. The parameters $\alpha_1^{(A)}$, $\alpha_4^{(A)}$, $\alpha_1^{(B)}$, and $\alpha_4^{(B)}$, which describe the vibrational dependence of the rotational constants, and the parameters $\overline{q}_4$, r_4, $\alpha_{14}^{(BB)}$, and $\alpha_{14}^{(AB)}$are obtained from the analysis of the stretching vibrational band system ν_1/ν_4 [41].

The H_{22} fundamental rovibrational parameters ($\alpha_1^{(A)}$, $\alpha_4^{(A)}$, $\alpha_1^{(B)}$, $\alpha_4^{(B)}$, $\alpha_{14}^{(BB)}$, $\alpha_{14}^{(AB)}$, $\overline{q}_4$, and r_4) have been calculated from the *ab initio* force field as follows. The H_{22} operator can be written in a general form [43] as

$$H_{22}/hc = \frac{1}{2}\sum_{\alpha,\beta} J_\alpha J_\beta \sum_{r,s} T_{rs}^{(ab)}\left(p_r p_s + q_r q_s\right), \tag{58}$$

where the summations in α and β are over molecule fixed cartesian axes x, y, and z and the summations in r and s are over the normal modes. The T coefficients

are functions of the structure and the harmonic and cubic force constants in the normal coordinate representation, q_r and q_s are the dimensionless normal coordinates of the rth and sth mode, and p_r and p_s are the conjugate momenta, respectively. The H_{22} coefficients of this work are related to the T coefficients as

$$\begin{aligned}
\alpha_1^{(A)} &= -T_{11}^{(zz)} \\
\alpha_1^{(B)} &= -T_{11}^{(xx)} \\
\alpha_4^{(A)} &= -\frac{1}{2}\left(T_{4a4a}^{(zz)} + T_{4b4b}^{(zz)}\right) \\
\alpha_4^{(B)} &= -\frac{1}{4}\left(T_{4a4a}^{(xx)} + T_{4b4b}^{(xx)} + T_{4a4a}^{(yy)} + T_{4b4b}^{(yy)}\right) \\
\overline{q}_4 &= -\frac{1}{2}\left(T_{4a4a}^{(xx)} - T_{4b4b}^{(xx)} + T_{4a4b}^{(xy)} + T_{4a4b}^{(yx)}\right) \\
r_4 &= \frac{1}{8}\left(T_{4a4a}^{(xz)} - T_{4b4b}^{(xz)} - T_{4a4b}^{(yz)} - T_{4a4b}^{(zy)}\right) \\
\alpha_{14}^{(AB)} &= \frac{1}{2}\left(T_{14a}^{(xz)} - T_{14a}^{(zx)} + T_{14b}^{(yz)} + T_{14b}^{(zy)}\right) \\
\alpha_{14}^{(BB)} &= \frac{1}{2}\left(T_{14a}^{(xx)} - T_{14a}^{(yy)} + T_{14b}^{(xy)} + T_{14b}^{(yx)}\right).
\end{aligned} \tag{59}$$

The program Spectro [29] has been used to calculate T coefficients. The numerical values obtained for the spectroscopic parameters are presented in the page 8852 of the Paper 3. Using these results, the effective parameters of Eqs. (56) and (57) can be calculated (see page 8853 in Paper 3). The final results show that the experimental data for the n = 2, 3, 4, and (with some limitations) 6 states (see Table V in Paper 3) are in good agreement with the *ab initio* values.

Finally, $A_0 - A_{n00}$ and $B_0 - B_{n00}$ (see page 8853 in Paper 3) can be calculated from the *ab initio* values of Hamiltonial parameters of Eqs. (59). Again, theoretical values agree well with the experimental results (see Table V in Paper 3), only the value of $(B_0 - B_{600})$ not fitting well.

5.2 Correctio ns to the metric tensor elements of NH_3, PH_3, AsH_3, SbH_3, and BiH_3 in the precence of bond angle constraints

Vibrational kinetic energy coefficients have been calculated for pyramidal symmetric top molecules NH_3, PH_3, AsH_3, SbH_3, and BiH_3, which are close to the local mode limit. The starting point is the stretching vibrational Hamiltonian

[8, 44]

$$H/hc = \sum_{i=1}^{3} \left(\frac{1}{hc} g^{(rr)} p_i^2 + D_e y_i^2 \right) + \sum_{i<j} \left(\frac{1}{hc} g^{(rr')} p_i p_j + f_{rr'} a_r^{-2} y_i y_j \right), \qquad (60)$$

where $y_i = 1 - e^{-a_r \Delta r_i}$ is the Morse variable and Δr_i is the bond stretching diplacement coordinate. The weight function for integration associated with this Hamiltonian is equal to one.

In the model Hamiltonian, bond angle coordinates are frozen to the equilibrium value. The role of constraints is controversial in quantum mechanics [45] but the solution is known in classical mechanics for present types of vibrational problems. When considering these rigid constraints, the Hamiltonian is modified as follows. The vibrational metric tensor elements $g_C^{(ij)}$ in the precence of rigid constraints can be obtained from the unconstrained elements $g^{(ij)}$ as [10]

$$g_C^{(rr)} = g^{(rr)} - \sum_{i=1}^{3} \sum_{j=1}^{3} g^{(r\theta_i)} M_{ij} g^{(r\theta_j)} \qquad (61)$$

$$g_C^{(rr')} = g^{(rr')} - \sum_{i=1}^{3} \sum_{j=1}^{3} g^{(r\theta_i)} M_{ij} g^{(r'\theta_j)}, \qquad (62)$$

where the indices i and j are over the three constrained bending degrees of freedom ($\Delta\theta_1, \Delta\theta_2,$ and $\Delta\theta_3$ being the appropriate displacement coordinates) and M_{ij} is an element of the symmetric matrix

$$M = \begin{pmatrix} g^{(\theta_1\theta_1)} & g^{(\theta_1\theta_2)} & g^{(\theta_1\theta_3)} \\ g^{(\theta_1\theta_2)} & g^{(\theta_2\theta_2)} & g^{(\theta_2\theta_3)} \\ g^{(\theta_1\theta_3)} & g^{(\theta_2\theta_3)} & g^{(\theta_3\theta_3)} \end{pmatrix}^{-1} . \qquad (63)$$

All unconstrained tensor elements can be obtained from Ref. [10].

I have calculated the constrained and unconstrained stretching vibrational metric tensor elements for NH_3, PH_3, AsH_3, SbH_3, and BiH_3. The results are gathered in Table IV of Paper 5. It is clear that when the mass of the central atom is large and the bond angles are close to 90^o, for example, in the case of BiH_3, there is no real difference whether constrained or unconstrained metric tensor elements are used in Eq. (60).

The eigenvalues of the vibrational Hamiltonian in Eq. (60) with the unconstrained metric tensor elements have been calculated for bismutine, BiH_3. Calculations have been carried variationally with a symmetrized Morse oscillator

product basis. All matrix elements have been obtained with analytic formulas. All basis functions with the maximum stretching quantum number 6 have been included. The non-linear least squares method has been employed to optimize the harmonic wave number ω_r, the anharmonicity constant x_{rr}, and $f_{rr'}$ instead of the true potential energy parameters D_e, a_r, and $f_{rr'}$ in order to reduce correlation between the parameters. However, this is not a problem because simple relations between ω and ωx, and D_e and a_r allow to convert one parameter set to the other [8]. Experimental vibrational term values have been employed as data. For bismutine, the parameter values obtained are $\omega_r = 1795.65$ (66) cm^{-1}, $x_{rr} = -30.78$ (23) cm^{-1}, and $f_{rr'} = -42.0$ (179) cm^{-1}Å^{-2}. The uncertainties in the parentheses are one-standard deviations in the least significant digit. The fit to the experimental vibrational term values is given in Table V of Paper 5. The standard deviation of the fit obtained is 0.28 cm^{-1}. It is clear that the model accounts well for the observed vibrational term values, and the stretching potential energy parameters obtained are true values.

6 Conclusions

Theoretical electronic structure calculation methods provide a powerful tool in modelling vibrational spectra even for a challenging molecule like methanol which shows complicated band structures in the overtone regions. A quartic force field for methanol has been computed and successfully applied in calculating spectra and spectroscopic parameters. A curvilinear internal coordinate Hamiltonian provides a simple physical picture (in practice this means fewer model parameters with an intuitive physical interpretation) and is well suitable to model stretching-torsion interactions. The normal coordinate approach is a practical method to calculate vibrational spectra by employing a computed *ab initio* force field. With these methods, most of the spectral structures can be systematically explained. However, more theoretical and experimental work is still required. For example, coupling between the torsion and bendings in the methyl group has not been modelled. Unfortunately my simple approach to the torsion-stretching coupling cannot be directly adopted to this problem. One possible solution is to employ the symmetry coordinates of Eqs. (1) - (12) for the bending degrees of freedom.

The rotational structure of the vibrational stretching overtones ($n00A_1/E$, $n = 3$, 4, and 6) of H_3SiD have been successfully analyzed with the normal and

local mode models. *Ab initio* results have been applied to determine Hamiltonian parameters for the excited states. Results from electronic structure calculations with a simple local mode interpretation of some vibration-rotation parameters turned out to be a crucial step in the rotational analysis of the spectra.

A vibrational analysis of BiH_3 using a simple stretching vibrational local mode model produces good results. The model takes into account corrections to the stretching vibrational metric tensor in the presence of the rigid constraints in the bending vibrations. Due to small kinetic energy coupling between the stretching and bending oscillators in BiH_3, these corrections are found to be neglible. The aim of this work is to study the implications of employing constraints in the vibrational models. It is pleasing that good results can be obtained while setting constraints to some degrees of freedom. For example, this approach can be applied to the study of internal motions in larger systems where at least at the moment it is practically impossible to employ excact calculations.

In future, as a consequence of development of computers, potential energy surfaces can be calculated accurately for larger molecules. These systems contain many different types of internal degrees of freedom, including large amplitude motions. I hope that my approach to treat large amplitude motion in methanol will help in finding effective theoretical methods to model nuclear motions in these systems.

Acknowledgement 1 *I want to express my gratitude to the supervisor of my thesis, Prof. Lauri Halonen, who has provided me good working facilities, knowledgeable advice, and free working environment. Without his constant support, I would have been unable to complete this study.*

I wish to thank all the members of the Laboratory of Physical Chemistry for a wonderful atmosphere. Especially, for the scientific part, I am grateful to my colleagues Janne Pesonen, Andrea Miani, and Mathias Horn.

Financial support from The Graduate School Laskemo (Ministry of Education), Magnus Ehrnrooth Foundation, and the Cultural Foundation of Finland, is gratefully acknowledged. CSC Limited (Espoo) is thanked for computer time.

I thank my parents Rauno and Hilkka for their valuable support.

This thesis is dedicated to my loved ones Alvari, Miska, and Tuulia.

References

[1] R. Khrisnan and J. A. Pople, Int. J. Quant. Chem. **14**, 91 (1978).

[2] K. Raghavachari, G. W. Trucks, J. A. Pople, and M. Head-Gordon, Chem. Phys. Letters, **157**, 479 (1989).

[3] K. K. Lehmann, G. Scoles, and B. H. Pate, Annu. Rev. Phys. Chem. **45,** 241 (1994).

[4] D. J. Nesbitt and R. W. Field, J. Phys. Chem. **100,** 12735 (1996).

[5] G. Herzberg, *Molecular Spectra and Molecular Structure,* Vol II, *Infrared and Raman Spectra,* New York: Van Nostrand (1945).

[6] B. R. Henry, In *Vibrational Spectra and Structure*, edited by J. R. Durig (Elsevier, New York, 1981), Vol. 10.

[7] M. S. Child and L. Halonen, Adv. Chem. Phys. **57**, 1 (1984).

[8] L. Halonen, Adv. Chem. Phys. **104**, 41 (1998).

[9] X. Wang and D. S. Perry, J. Chem. Phys. **109**, 10795 (1998).

[10] E. B. Wilson, J. C. Decius, and P. C. Cross, *Molecular Vibrations* (Dover, New York, 1980).

[11] L. Lubich, O. V. Boyarkin, R. D. F. Settle, D. S. Perry, and T. R. Rizzo, Faraday Discuss. Chem. Soc. **102**, 165 (1995).

[12] O. V. Boyarkin, L. Lubich, R. D. F. Settle, D. S. Perry, and T. R. Rizzo, J. Chem. Phys. **107**, 8409 (1997).

[13] O. V. Boyarkin, L. Lubich, R. D. F. Settle, D. S. Perry, and T. R. Rizzo, J. Chem. Phys. **110**, 11346 (1999).

[14] O. V. Boyarkin, L. Lubich, R. D. F. Settle, D. S. Perry, and T. R. Rizzo, J. Chem. Phys. **119**, 11359 (1999).

[15] R. A. Kendall, T. H. Dunning Jr., and R. J. Harrison, J. Chem. Phys. **96**, 6769 (1992).

[16] T. H. Dunning Jr., J. Chem. Phys. **90**, 1007 (1989).

[17] R. T. Lawton and M. S. Child, Mol. Phys. **40**, 773 (1980).

[18] M. S. Child and R. T. Lawton, Faraday Discuss. Chem. Soc. **71**, 273 (1981).

[19] D. Papousek and M. R. Aliev, *Molecular Vibrational-Rotational Spectra* (Elsevier, Amsterdam, 1972).

[20] O. Vaittinen, M. Saarinen, L. Halonen, and I. M. Mills, J. Chem. Phys. **99**, 3277 (1993).

[21] A. Willetts and N. C. Handy, Spectrochim. Acta, **53**, 1169 (1997).

[22] B. T. Darling and D. M. Dennison, Phys. Rev. **57**, 128 (1940).

[23] I. M. Mills, *Molecular Spectroscopy: Modern Research*, edited by K. N. Rao and C.-W. Matthews (Academic Press, New York, 1972), Vol. I.; I. M. Mills, *Specialist Periodical Report, Theoretical Chemistry*, edited by R. N. Nixon, (The Chemical Society, London, 1974), Vol. I.

[24] M. M. Law, Ph.D. thesis, University of Aberdeen, Scotland (1992).

[25] K. K. Lehmann, Mol. Phys. **66**, 1129 (1989).

[26] K. K. Lehmann, Mol. Phys. **75**, 739 (1992).

[27] P. M. Morse, Phys. Rev. **34**, 57 (1929).

[28] A. R. Hoy, I. M. Mills, and G. Strey, Mol. Phys., **24**. 1265 (1972).

[29] J. F. Gaw, A. Willets, W. H. Green, and N. C. Handy, *Advances in Molecular Vibrations and Collision Dynamics*, edited by J. M. Bowman, (JAI Press, Greenwich,1990).

[30] R. H. Hunt, W. N. Shelton, F. A. Flaherty, and W. B. Cook, J. Mol. Spectrosc. **192**, 277 (1998).

[31] L.-H. Xu, X. Wang, T. J. Cronin, D. S. Perry, G. T. Fraser, and A. S. Pine, J. Mol. Spectrosc. **185**, 158 (1997).

[32] A. Serrallach, R. Meyer, and Hs. H. Günthard, J. Molec. Spectrosc. **52**, 94 (1974).

[33] D. Rueda, *Overtone Spectroscopy of Methanol: Global Vibrational Analysis and Vibrational Dependence of the Torsional Potential.* Doctoral Thesis No. 2438, Ecole Polytechnique Federale de Lausanne, Switzerland (2001).

[34] L. Halonen, J. Chem. Phys. **106**, 7931 (1997).

[35] I. M. Mills, Faraday Discuss. Chem. Soc. **102**, 244 (1995).

[36] L. Halonen and A. G. Robiette, J. Chem. Phys. **84**, 6861 (1986).

[37] M. Halonen, L. Halonen, H. Bürger, and P. Moritz, J. Chem. Phys. **95**, 7099 (1991); Chem. Phys. Lett. **203**, 157 (1993).

[38] I. M. Mills and A. G. Robiette, *Mol. Phys.* **56**, 743 (1985).

[39] L. S. Bartell, D. J. Romanesko, and T. C. Wong, in *Specialist Periodical Report, Molecular Structure by Diffraction Methods*, edited by G. A. Sim and L. E. Sutton (The Chemical Society, London, 1975), Vol. 3.

[40] T. Lukka and L. Halonen, J. Chem. Phys. **101**, 8380 (1994).

[41] G. Graner, O. Polanz, H. Bürger, H. Ruland, and P. Pracna, J. Mol. Spectrosc. **188**, 115 (1998).

[42] H. Bürger, H. Ruland, and L. Halonen, J. Mol. Spectrosc. **182**, 195 (1997).

[43] M. R. Aliev and J. K. G. Watson, in *Molecular Spectroscopy: Modern Research*, edited by K. N. Rao (Academic, New York, 1985), Vol. III.

[44] L. Halonen and M. S. Child, J. Chem. Phys. **79**, 4355 (1983).

[45] J. Pesonen and L. Halonen, Adv. Chem. Phys. **125**, 269 (2003).